Rev.Adv.Mater.Sci. 20(2009) 21-27

ADSORPTION PROPERTIES OF CARBON NANOTUBES FROM MOLECULAR DYNAMICS VIEWPOINT

Viatcheslav V. Barkaline and Alexander S. Chashynski

Systems Dynamics & Materials Mechanics Laboratory, Belarusian National Technical University, Nezavisimosti ave, 65, Minsk, 220013, Belarus

Received: February 03, 2008

Abstract. Results of molecular dynamics simulation of adsorption properties of nanostructured carbon material are presented. Interaction of various small and large molecules with graphite, graphene layer, carbon nanotubes, and their bundles are studied. Selective permittivity both of single tube and tubes' bundles depending on their structures is demonstrated. Nanotube electronic density redistribution under the covalent functional modification of nanotubes is analyzed. Role of rings in adsorbate chemical structures is studied from the viewpoint of adsorption energy. Effect of one chain DNA immobilization on carbon nanotube arrays is discussed. Multiwall carbon nanotubes of various structures are simulated to determine optimal ones and multilayer contribution to adsorption energy.

1. INTRODUCTION

Possible use of nanostructured carbon materials as gas molecules adsorbents attracts much attention at present due to high values of adsorbing area and sensitivity of such materials properties to adsorbed molecules [1]**.** Such materials usually contain the variety of carbon phases (carbon nanotubes (CNT), graphene layers, graphite inclusions, and other). Selectivity of nanostructured carbon adsorbents depends crucially on chemical functionalization of structure elements of these materials [2]. The ordered carbon nanotube arrays seem to be most promising from the viewpoint of gas sensors with acoustic output [3]**.** The design of such sensors needs study of adsorption properties of single and multiple wall CNT and their bundles. In the present paper we propose the results of molecular dynamics (MD) study of them. CNT interaction with DNA molecules and dioxins are also discussed.

2. INTERATOMIC POTENTIAL MM+

The absence of spatial periodicity in nanoscale molecular systems leads to the necessity to develop models with specific atom-atom interactions. One approach treats all interactions as fundamentally pair-wise with electrostatic interaction modified by some short-range repulsion terms. This type of models is appropriate for ionic solids. Alternatively, valence force-field models appropriated for covalent molecules are used with interatomic potentials including many-body terms to account for the directionality of covalent bonds. It requires knowledge of force constants specific for the certain chemical environment. Because its variety rises, the number of force constants becomes very large. It is very useful to have a general model that, even if it is less accurate, makes it possible to obtain results even if not all force constants are known. Such model is embedded to MM+ valence force field [4,5] with optimized default values of

Corresponding author: Viatcheslav V. Barkaline, e-mail: barkaline@bntu.by

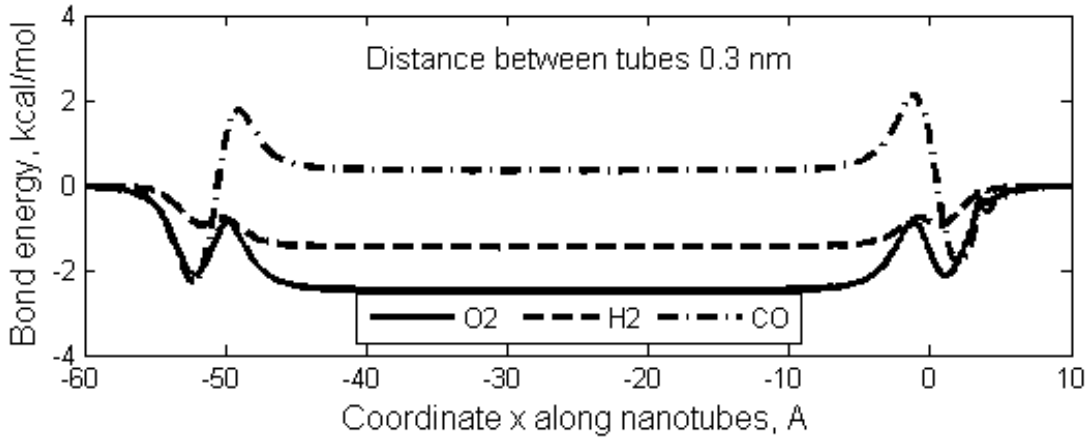

Fig. 1. Adsorption energy of gas molecules in the centres of pores in CNT array versus coordinate along pore.

force constants. Valence force-fields describe both bonding and non-bonding interactions. Bonding interactions usually refer to atoms which are or directly bonded (bond stretch relationship), or geminal to each other (angle bending relationship), or vicinal to each other (dihedral angle relationship). The non-bonding interactions include the exchange repulsion when atoms are too close, a long-range attraction arising from dispersion forces, and electrostatic interactions coming from the interaction of charges and multipoles.

Angle Bending. This term is associated with the deformation of an angle between bonds from its normal value. The angle bending term in MM+ is

$$V_{angle} = \frac{1}{2}\sum_{\substack{bond\\angles}} K_\theta \left(\theta - \theta_0\right)^2 \left[1 + C_\theta \left(\theta - \theta_0\right)^4\right]. \quad (1)$$

The default value of C_θ is 7.0×10^{-8} deg^{-4}. MM+ uses special values for the bending force constants K_θ when the atoms are in a three- or four-membered rings.

Bond Stretching. This term is associated with deformation of every chemical bond from its standard equilibrium length r_0 to r. MM+ uses a cubic stretch term

$$V_{bond} = \frac{1}{2}\sum_{\substack{i,j\in\\bonds}} K_r^{ij}\left(r_{ij} + r_{ij}^0\right)^2 \left[1 + \delta\left(r_{ij} - r_{ij}^0, \frac{1}{3}C_S^{ij}, \frac{4}{3}C_S^{ij}\right)\cdot C_S^{ij}\cdot\left(r_{ij} - r_{ij}^0\right)\right], \quad (2)$$

where K_r is the current bond force constant and C_S – its anharmonicity parameter. The default value is C_S = -2.0 (if r and r_0 are in Å). Switching function δ is introduced for vanishing cubic term on large bond stretches:

$$\delta(x,a,b) = \begin{cases} 1, x \le a \\ 0, x \ge b \\ \dfrac{(b-x)^2(b+2x-3a)}{(b-a)^3}, a < x < b \end{cases}. \quad (3)$$

Bond Dipoles. In MM+ the electrostatic contribution comes from a set of bond dipole moments associated with polar bonds. The center of the dipole is defined to be the midpoint of the bond and two dipoles μ_i and μ_j separated by r_{ij} are associated with bond. The MM+ dipole energy is

$$V_{dipole} = \frac{\varepsilon}{2}\sum_{\substack{ij\in\\bond}} \mu_i\mu_j \frac{\cos\chi - \cos\alpha_i \cos\alpha_j}{r_{ij}^3}, \quad (4)$$

where dielectric constant ε has the default value 1.5. χ is the angle between two dipole vectors, α_i and α_j are the angles that the dipole vectors make with the $\boldsymbol{r}_{ij}$ vector.

Bond Stretch and Angle Bending Cross Term. MM+ includes coupling between bond stretching and angle bending. If the angle including atoms *i,j,* and *k*, where *k* is the central atom;

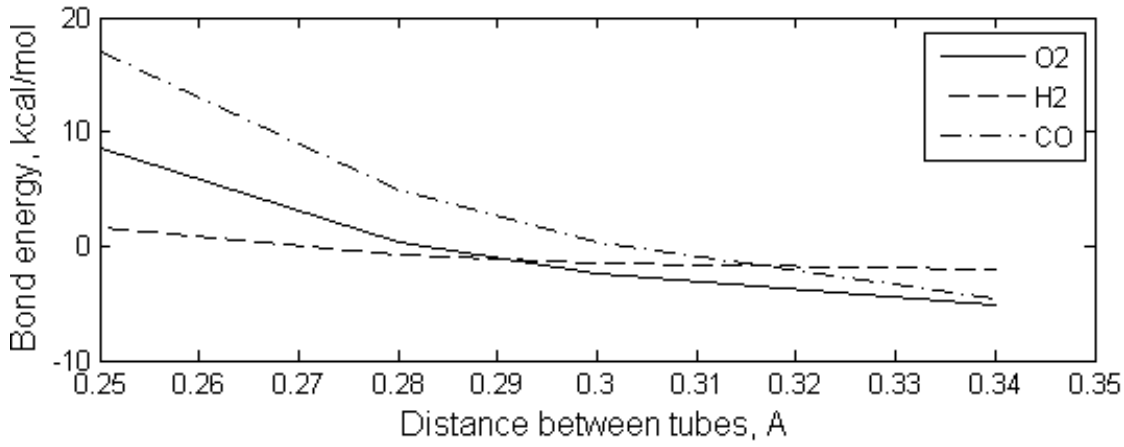

Fig. 2. Adsorption minima of gas molecules in the pores of ordered CNT array versus minimal intertube gap.

then MM+ couples stretching of the *ik* and *jk* bonds with the angle:

$$V_{stretch-bend} = \sum_{\substack{bond\\ angles\ ikj}} K_{sb}\left(\theta-\theta_0\right)_{ikj} \cdot \left[\left(r-r_0\right)_{ik}+\left(r-r_0\right)_{ik}\right]. \quad (5)$$

If *R* is an atom other than hydrogen, the values of the stretch-bend force constants are: K_{sb} =0.120 for XR_2, K_{sb} =0.090 for *XRH*, *X* = atom in 1st long row or K_{sb} =0.250 for XR_2, K_{sb} =- 0.400 for *XRH*, *X* = atom in 2nd long row.

Out-of-Plane Bending. An atom that has sp^2 hybridization tends to be coplanar with its attached atoms. This effect is accounted for by out-of-plane-bending interactions in MM+. Consider the situation involving an atom *X* that is sp^2 hybridized. *Y* is the projection of *X* onto the *ABC* plane. The angle bending calculations are modified to use the in-plane angles *AYB*, *AYC*, and *BYC* in Eq. (5) with the standard force constants rather than the standard angles *AXB*, *AXC*, and *BXC*. In addition, out-of-plane components are computed as well, for the out-of-plane angles *XAY*, *XBY*, and *XCY*. These last three calculations use Eq. (5) as well, but with a θ_0 equal to 0 and special out-of-plane bending force constants.

Dihedrals. This term is associated with the tendency of dihedral angles to have a certain *n*-fold symmetry and to have minimum energy for the *cis*-, *gauche*-, or *trans*-conformation, etc.

$$V_{gihedral} = \frac{1}{2}\sum_{dihedrals} V_n\left[1+\cos\left(n\varphi-\varphi_0\right)\right]. \quad (6)$$

The period of the interaction is 360/*n*. For *n*=1 and φ_0=0 the term represents the situation where the energy is minimal the *trans*-conformation with a barrier of V_n to the highest energy *cis*-conformation. A phase angle of φ_0=180° represents the opposite situation. *n* is restricted to values from 1 to 6, so up to six Fourier terms may be used for a particular dihedral angle.

Van der Waals. The MM+ van der Waals interactions combine an exponential repulsion with an attractive $1/R^6$ dispersion interaction. The basic parameters are a van der Waals radius r_i^* for each atom type and a hardness parameter ε_i that determines the depth of the attractive well and how easy or difficult it is to push atoms close together. There are interactions for each non-bonded *ij*-pair. The parameters for a pair are obtained from individual atom parameters as $r_{ij}^* = r_i^* - r_j^*$, $\varepsilon_{ij} = \sqrt{\varepsilon_i \cdot \varepsilon_j}$. Van der Waals interaction is then calculated as

$$V_{vdW} = \sum_{ij-pairs} \varepsilon_{ij}\left(A_{ij}e^{-\alpha\rho_{ij}} - B_{ij}\rho_{ij}^{-6}\right), \quad (7)$$

where $\rho_{ij} = r_{ij} / r_{ij}^*$.

3. RESULTS AND DISCUSSION

Adsorption properties of CNT bundles. Previous investigations showed that majority of small molecules have adsorption minima in CNT array not inside CNT but in intertube pores while intertube distance is small enough. These minima were calculated for O_2, H_2, and CO molecules and presented on Fig. 1 for (10,10) CNT array (tube diam-

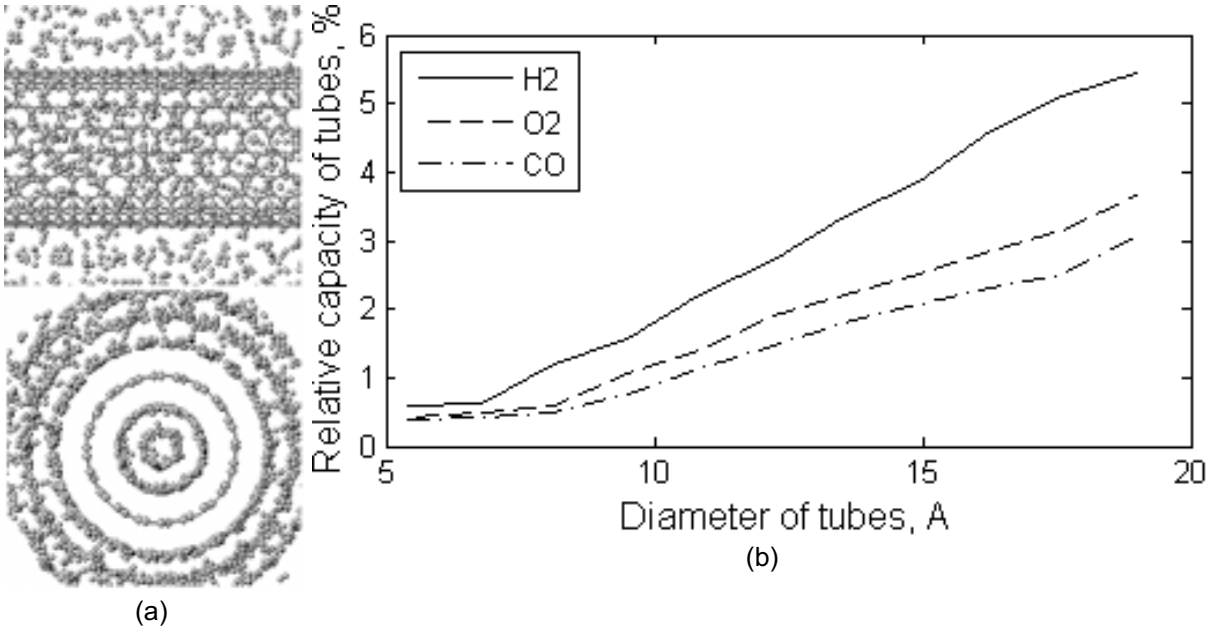

Fig. 3. H_2 filling of CNT (6,6) (a) and CNT absorption capacity dependence on its diameter (b).

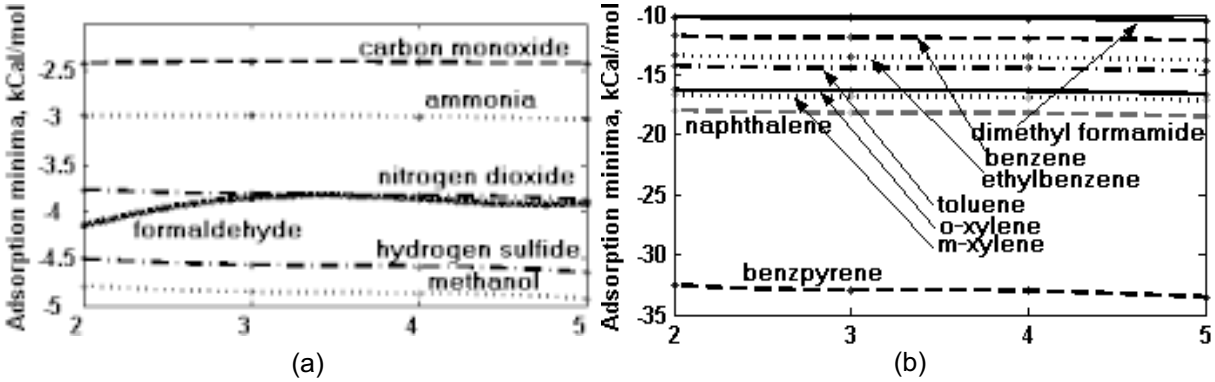

Fig. 4. Adsorbtion minima for external surface of MWNT ($D_{external}$ = 40 nm) versus number of layers.

eter D=13.56 Å, intertube distance 3.4 Å). Tubes were closed from one side by appropriate fullerene caps. Penetration of gas molecules throughout pores is determined by relationship between molecule and pore sizes. When pores are small molecules have positive potential energy in pores and leave them. Fig. 2 shows that this effect can be used for separation of various molecules. Critical intertube distance is r≈3 Å for CO, 2.8 Å for O_2, and 2.7 Å for H_2 .

When CNT has open ends, they absorb gas molecules into their internal areas. During simulation CNT with various diameters were taken and obduced by the cloud of molecules. Then steady state of whole system was obtained using MD optimization and relation of the number of adsorbed molecules in this state and carbon atoms number was determined (absorption capacity of CNT). Absorbed molecules in CNT are distributed regularly and create internal layers and other ordered structures when CNT diameter rises (Fig. 3a). Fig. 3b shows absorption capacity of CNT versus tube diameter for H_2, O_2, and CO gases.

Adsorption properties of multiwall CNT. Multiwall CNTs (MWNT) are the main subject in the development of the technology of ordered CNT arrays on various substrates. Ideal geometry of MWNT was obtained and optimized with respect to potential energy minima. Interlayer distance in MWNT is close to interplane graphite distance 3.4 Å and varies in the ±0.2 Å domain. Then two-atomic molecules can not penetrate into the MWNT wall and adsorption takes place at the external surface of MWNT. Dependence of adsorption energy on number of MWNT layers is weak (Fig. 4).

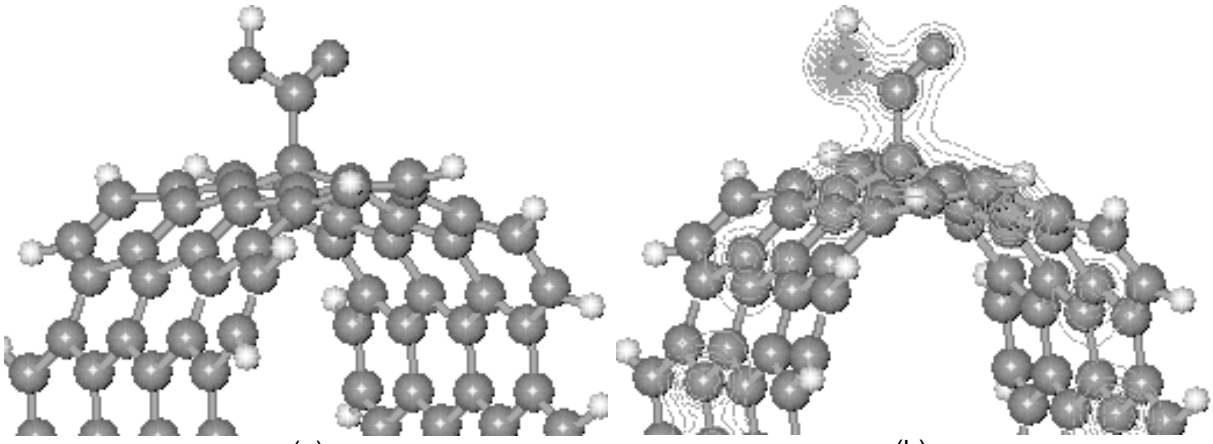

(a) (b)

Fig. 5. Carboxyl group bonded to CNT (a) and contour plot of electron density of functionalized CNT (b).

Table 1. Contribution of additional CNT-H bond to the energy of CNT–O–C_nH_{2n+1} bond.

Bond	Energy change, kCal/mole
CNT–O–CH_3	–66.04
CNT–O–C_2H_5	–65.38
CNT–O–C_3H_7	–65.33
CNT–O–C_4H_9	–65.32

Table 2. Structure of carboxylic group –COOH on CNT surface.

Bond	length, nm	Bond	Angle, deg.
C_{tube}–C	0.154	C_{tube} –C–O	116,4
C=O	0.122	C_{tube} –C=O	128,0
C–O	0.135	C–O–H	109,5
O–H	0.095	-	-

Some correlation exists there between chiralities of single wall nanotubes composing MWNT with minimal energy. For example, 5×5@10×10@15×15 and 2×7@10×10@15×15 MWNTs were studied. Bond energies for these tubes are 45.9 kCal/mole (2 eV) and 196.3 kCal/mole (8.52 eV) correspondingly. Single wall CNTs in MWNT may obey both commensurate and incommensurate longitudinal periods.

Functional modification of CNT. CNT functionalization by grafting of molecular fragments is based on the ability of their peripheral atoms to create chemical bonds with CNT carbon atoms which transform their hybridization state from sp^2 to sp^3. It is necessary to mark that aromatic type of bonds in CNT during that process transforms to alternating single and double bonds at the essential part of CNT. To localize such defect it is necessary to introduce, for example, atoms of hydrogen â to the vicinity of current bond. Electrical conductivity of CNT in this case will not change essentially.

Oxidation of CNT in solutions leads to covering of its external surface by carboxylic (–COOH), carbonyl (–CO) or hydroxyl (–OH) groups. Quantum mechanical calculations of interaction of –O–C_nH_{2n+1} groups with (6,6) CNT surface were undertaken using PM3 approach. Bond CNT–O–C_nH_{2n+1} creates center of 2D simulation cluster, containing 96 carbon atoms from the CNT surface area neighbor of the bond. Hydrogen atoms were attached to boundary atoms of the cluster for bond breaking compensation. To localize the effect of CNT–O–C_nH_{2n+1} bond on electronic properties of CNT hydrogen atom was bonded to carbon atom in the vicinity of the studied bond, then not one but two sp^3 bonds are created. Creating of additional bond leads to decreasing of the energy of system (Table 1).

Then CNT functionalization with carboxylic group –COOH was examined. Obtained Geometry of CNT–COOH bond is presented in Table 2. Carboxyl geometry change due to bonding to CNT is observed. Semiempiric PM3 data are in accor-

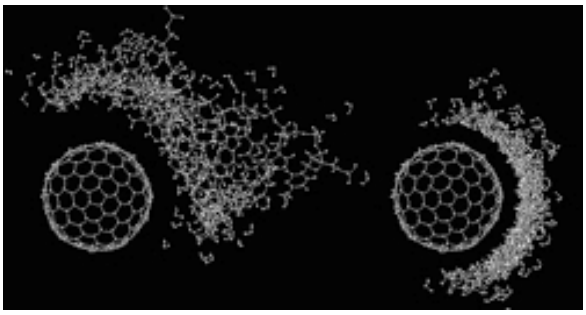

Fig. 6. DNA configuration change near (10,10) CNT (from left to right, 60 ps).

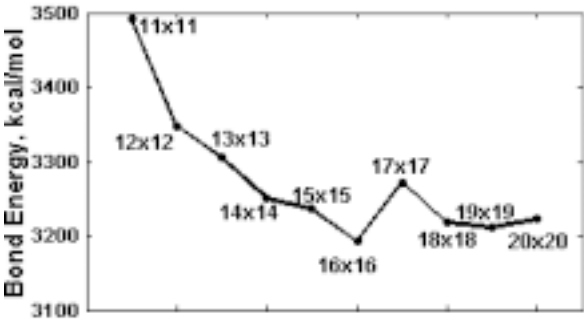

(a)

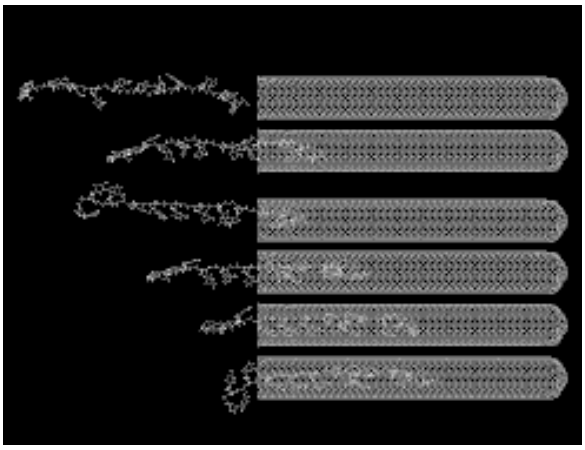

(b)

Fig. 7. Dependence of bond energy of one-chain DNA oligomer and CNT system on CNT chirality (a) and immobilization of one-chain DNA oligomer on 10x10 CNT: spontaneous retraction, from up to down(b).

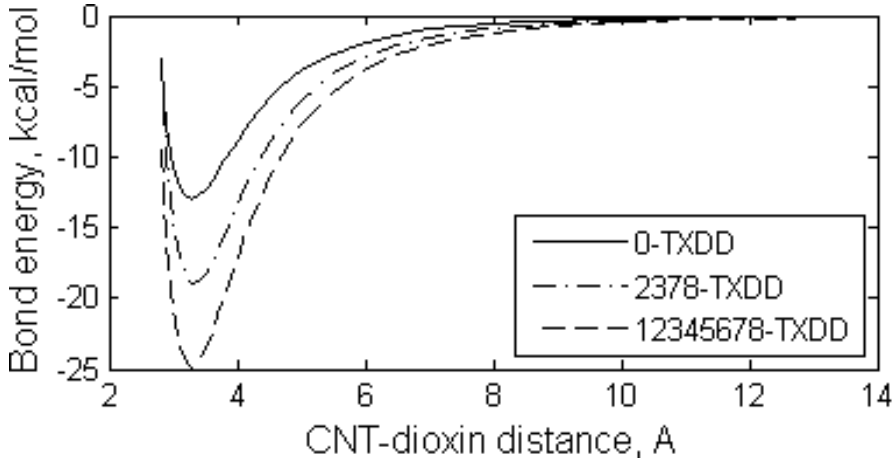

Fig. 8. Adsorption energies for CNT-dioxin systems.

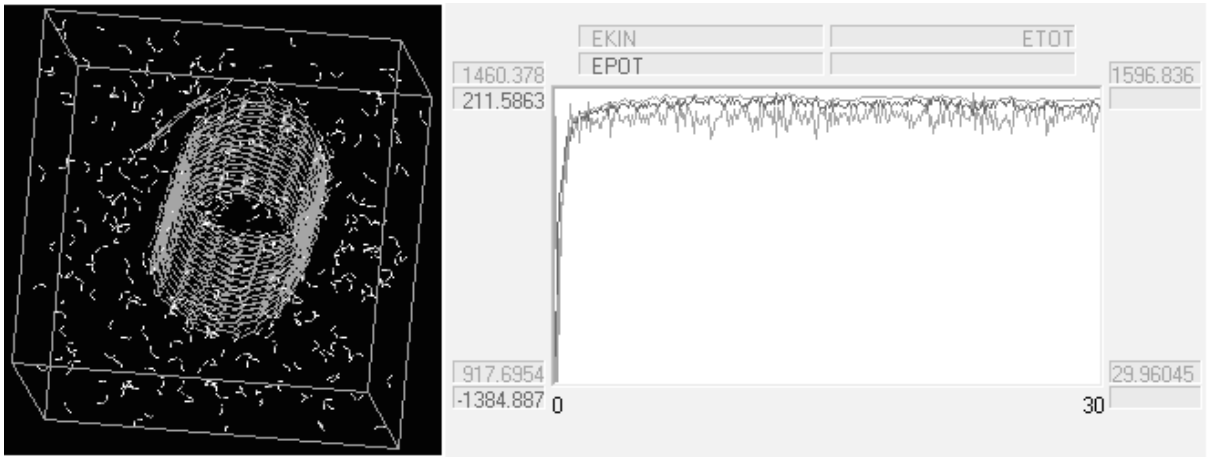

Fig. 9. CNT-dioxin system annealing in water: simulation periodic box (a), energy plots (b).

dance with ab initio DFT calculations. –COOH group leads to local deformation of tube wall due to erasing sp^3–hybridization defect (Fig. 5a). Electron density change (Fig. 5b) indicates the covalent bond creation.

DNA-CNT interaction. DNA oligomer and (10,10) CNT (*D*=13,56 Å) interaction was studied. Oligomer undergoes configuration change adsorbing on external surface of CNT (Fig. 6, simulation time period 60 ps). H-bonds in two-chain DNA structure can break near CNT leading to DNA denaturation up to one-chain oligomers. Character of DNA adsorption on internal surface of CNT depends crucially on CNT diameter (Fig. 7a). One chain DNA oligomer can spontaneously retract into CNT (Fig. 7b), this fact can be used in reversible DNA immobilization, the significant point in biosensorics [6].

CNT interaction with dioxins. Dioxins and dioxin-like compounds are global eco-toxicants with great mutagenic and carcinogenic effect. Dioxins have benzoic-like rings in their structures and then can strongly adsorb to CNT. Simulation of dibenzodioxin derivatives adsorption on (10,10) CNT was undertaken for determination of corresponding bond energies (Fig. 8). When chlorine content in dibenzodioxin derivatives rises the bond energy rises too. For instance, bond energy of 2,3,7,8–TXDD with CNT is 22.36 kCal/mole (0.97 eV), while that for 1,2,3,4,5,6,7,8–TXDD is 26.11 kCal/mole (1.13 eV). During annealing in water environment at 295K dioxin does not de-tack from the tube (Fig. 9).

4. CONCLUSION

Molecular dynamics approach is shown to be useful comparative studies of physical adsorption in various atomic-molecular systems with carbon nanotubes. Quantitative description needs pure quantum mechanical (QM) or mixed QM/MD simulation. Calculations with MM+ potential give understated estimates of adsorption energy because they do not account redistribution of electron density.

CNT are shown to be applicable as adsorbents of multi-atomic molecules such as DNA and other polymers.

Molecules having benzoic rings in their structures create sufficiently strong nonbonding links with CNT and could be used for noncovalent functionalizing of CNT in chemical sensor and water filter applications.

REFERENCES

[1] V. Barkaline and A. Chashynski, *Chemomechanical properties of ordered carbon nanotube arrays and their prospects in acoustic gas sensorics"*, In: *Physics, chemistry and application of nanostructures*, *Reviews and Notes to Nanomeeting 2007, Minsk, Belarus, 22-25 May, 2007,* ed. by V.E. Borisenko, S.V. Gaponenko and V.S. Gurin (World Scientific, 2007), p. 52.

[2] S. Banerjee, T. Hemraj-Benny and S.S. Wong // *Advanced Materials,* **17** (2005) 17.

[3] V.V. Barkaline, *Carbon nanotubes' arrays based Surface Acoustic Wave chemical sensor element*, In: *Proceedings of Eurosensors XIX International Conf*. (September 11-14, 2005, Barcelona, Spain).

[4] U. Burkert and N. L. Allinger, *Molecular Mechanics* (American Chemical Society Monograph 177, 1982).

[5] N.L. Allinger, *HyperChem Release 7 for Windows* (Hypercube, Inc., Publication HC70-00-01-00, January, 2002).

[6] S.S. Iqbal, M.W. Mayo, J.G. Bruno, B.V. Bronk, C.A.Batt and J.P. Chambers // *Biosensors & Bioelectronics* **15** (2000) 47.